

# Extracting the hadronization timescale in $\sqrt{s} = 7$ TeV proton-proton collisions from pion and kaon femtoscopy

T. J. Humanic

*Department of Physics, Ohio State University, Columbus, OH, USA*

---

## Abstract

A hadronic rescattering model with the proper hadronization time width as the free parameter is compared with charged pion and charged and neutral kaon femtoscopy measurements from the LHC ALICE experiment for  $\sqrt{s} = 7$  TeV proton-proton collisions. Comparisons between the model and measurements are made for one-dimensional source parameters in several charged multiplicity and transverse particle pair momentum bins. It is found that a reasonable description of the measured source parameters by the model is obtained for a hadronization proper time width of  $0.4 \pm 0.1$  fm/c, which is in agreement with an estimate based on the uncertainty principle. The model calculations also suggest that 1) some form of collectivity is necessary to describe the multiplicity dependence of the measured radius parameters, and 2) the underlying physical size and timescale of the collision is significantly larger than what the extracted radius parameters and hadronization proper time width would imply.

*Keywords:* 25.75.Dw., 25.75.Gz., 25.40.Ep

---

## 1. Introduction

Of fundamental interest in studying high-energy particle collisions is how hadrons are formed in these collisions. An important element in fully understanding the hadronization process is knowledge of the space-time position where the hadronization takes place during the collision. In proton-proton collisions, the spacial position of hadronization transverse to the collision axis is characterized by the radius of a proton, i.e. 1 fm, whereas the hadronization timescale and the longitudinal spacial position, which depends on the product of the longitudinal velocity and hadronization timescale, are not well

defined. An order-of-magnitude estimate for the hadronization proper time of a particle of rest mass  $m_0$  can be obtained by applying the uncertainty principle in the rest frame of the particle,

$$\Delta\tau \approx \frac{\hbar}{2\Delta E} \quad (1)$$

where  $\Delta E$  is the uncertainty in the particle energy and  $\Delta\tau$  is the uncertainty in the particle hadronization proper time, i.e. the width of the hadronization proper time distribution. Since Eq. 1 is evaluated in the rest frame of the particle, then  $\Delta E = \Delta m_0 \sim m_0$ , where  $\Delta m_0$  has been set to  $m_0$  as an order-of-magnitude estimate. Thus, Eq. 1 becomes,

$$\Delta\tau \approx \frac{\hbar}{2m_0} \leq 0.7 \text{ fm}/c \quad (2)$$

where, as the lightest hadron, the pion rest mass sets the upper limit on the width of the hadronization proper time distribution.

Several theoretical [1, 2] and phenomenological [3, 4, 5] studies of the hadronization (or formation) time in proton-proton collisions have been made over the past 30 years. The phenomenological ones have attempted to extract a single hadronization proper time in each case by comparing a model with two-pion femtoscopy measurements for  $\sqrt{s} = 0.2$  [3], 0.9 [4], and 1.8 [5] TeV collisions, obtaining values in the range of 0.1-0.2 fm/c. In a recent phenomenological study comparing the UrQMD model [6] with LHC ALICE collaboration 3-dimensional two-pion femtoscopy measurements in  $\sqrt{s} = 7$  TeV proton-proton collisions [7] a range for the single hadronization proper time of 0.3-0.8 fm/c was obtained. Although the extracted values in these studies are for  $\delta$ -function distributions of the hadronization proper time rather than widths of finite distributions, the extracted values seem consistent with the order-of-magnitude limit given in Eq. 2.

The main goal of the present work is to extract hadronization time information by comparing a rescattering model similar to that used in Refs. [3, 4, 5] with LHC ALICE 1-dimensional  $\pi^{ch}\pi^{ch}$ ,  $K^{ch}K^{ch}$ , and  $K_s^0K_s^0$  femtoscopy measurements in  $\sqrt{s} = 7$  TeV proton-proton collisions [7, 8, 9]. The main differences between the present work and the previous ones are the following:

- Rather than using a single hadronization proper time, a more physically motivated Gaussian distribution of proper times characterized by a

width,  $\tau_{had}$ , is used in the present work, as in Ref. [1].  $\tau_{had}$  will be more directly comparable with  $\Delta\tau$  in Eq. 2.

- The present rescattering model uses identified charges and anti-particles, rather than being isospin averaged as in the previous works, and also includes  $p\bar{p}$  and  $n\bar{n}$  annihilation,
- Rather than only making model comparisons with two-pion femtoscopy measurements, the present work will also compare with charged and neutral kaon measurements. This should serve to place additional constraint on the extracted hadronization proper time information.

The remainder of the paper is organized into a description of the model, results and discussion, and the summary.

## 2. Description of the model

The rescattering model used is similar to that used in Refs. [3, 4, 5] and is briefly described here. The PYTHIA version 6.4 code [10] is used to generate the initial particles and their momenta for  $\sqrt{s} = 7$  TeV proton-proton collisions. This version of PYTHIA has been found by the LHC ATLAS [11] and CMS [12, 13] collaborations to describe the measured pion and charged and neutral kaon transverse momentum distributions from  $\sqrt{s} = 7$  TeV proton-proton collisions reasonably well. Also, the ALICE collaboration has used a version of PYTHIA to model the correlation function backgrounds in its pion and charged and neutral kaon femtoscopy measurements in  $\sqrt{s} = 7$  TeV proton-proton collisions [7, 8, 9]. The particles extracted from PYTHIA and input into the model, including all charge states and anti-particles, are  $p, n, \pi, K, K^*, \Lambda, \Delta, \rho, \omega, \eta, \eta'$  and  $\phi$ . The allowed two-body scattering processes and decays, which are constrained to obey conservation of energy, momentum, charge, baryon and strangeness number, are:

- elastic ( $X$  and  $Y$  represent any particles)

$$XY \rightarrow XY$$

- inelastic and decays ( $N$  here represents a nucleon or anti-nucleon)

$$\begin{aligned} \pi N &\rightleftharpoons \Delta, \pi\Delta, K\Lambda & NN &\rightleftharpoons N\Delta & KN &\rightleftharpoons \pi\Lambda \\ \pi K &\rightleftharpoons K^* & \pi\pi &\rightleftharpoons \rho, \eta & \pi\pi &\rightarrow \phi \rightleftharpoons KK \\ \pi\pi &\rightarrow \omega, \eta' & \eta' &\rightarrow \pi\pi\pi & \Lambda &\rightarrow \pi N \end{aligned}$$

- $N\bar{N}$  annihilation

$$N\bar{N} \rightarrow \rho\rho, \rho\omega, \omega\omega, \rho\eta, \omega\eta, \eta\eta \quad (3)$$

The annihilation cross sections were taken from Ref. [14] and branching ratios from Ref. [15].

The space-time point of the  $i^{\text{th}}$  particle of rest mass  $m_{0i}$  at hadronization in the proton-proton collision frame  $(x_i, y_i, z_i, t_i)$  with PYTHIA energy-momentum  $(p_{xi}, p_{yi}, p_{zi}, E_i)$  is determined in the model by a Gaussian distribution for the transverse radius,  $r_T$ , and, as mentioned earlier, a Gaussian distribution for the proper time,  $\tau$ , such that

$$\frac{dn}{dr_{Ti}} \propto \exp\left(-\frac{r_{Ti}^2}{2\sigma_r^2}\right) \quad \frac{dn}{d\tau_i} \propto \exp\left(-\frac{\tau_i^2}{2\tau_{had}^2}\right) \quad (4)$$

$$x_i = r_{Ti} \cos \phi_i \quad y_i = r_{Ti} \sin \phi_i \quad z_i = \tau_i \frac{p_{zi}}{m_{0i}} \quad t_i = \tau_i \frac{E_i}{m_{0i}} \quad (5)$$

where  $\sigma_r$  is set to 1 fm,  $\phi_i$  is the azimuthal angle of the  $i^{\text{th}}$  particle set randomly between  $0 - 2\pi$ , and  $\tau_{had}$  is the hadronization proper time width, which is a free parameter to be adjusted to get the best agreement with measurements.

Each particle is allowed to evolve from these initial conditions in time steps of 0.25 fm/c undergoing scatterings and decays until no more scatterings or decays occur. At this point, freeze-out of the particle occurs and after this point the particle is free streaming.

Quantum statistics is imposed pair-wise on boson pairs  $a$  and  $b$  by weighting them at their freeze-out phase-space points  $(\vec{r}_a^\rightarrow, t_a, \vec{p}_a^\rightarrow, E_a)$  and  $(\vec{r}_b^\rightarrow, t_b, \vec{p}_b^\rightarrow, E_b)$  with

$$W_{ab} = 1 + \cos(\Delta\vec{r}^\rightarrow \cdot \Delta\vec{p}^\rightarrow - \Delta t \Delta E) \quad (6)$$

where,

$$\Delta\vec{r}^\rightarrow = \vec{r}_a^\rightarrow - \vec{r}_b^\rightarrow \quad \Delta\vec{p}^\rightarrow = \vec{p}_a^\rightarrow - \vec{p}_b^\rightarrow \quad \Delta t = t_a - t_b \quad \Delta E = E_a - E_b \quad (7)$$

The correlation function,  $C(q_{inv})$ , is formed by binning pairs in terms of the invariant momentum difference  $q_{inv} = |\Delta\vec{p}^\rightarrow| - |\Delta E|$  as the ratio of weighted pairs,  $N(q_{inv})$ , to unweighted pairs,  $D(q_{inv})$ ,

$$C(q_{inv}) = \frac{N(q_{inv})}{D(q_{inv})} \quad (8)$$

Since there are no final-state interactions in the model between boson pairs after freeze out such as Coulomb or strong interactions, a simple Gaussian function is fitted to Eq.8 to extract the boson source parameters which are compared with experiment,

$$C_{\text{fit}}(q_{\text{inv}}) = \alpha[1 + \lambda \exp(-q_{\text{inv}}^2 R^2)] \quad (9)$$

where  $R$  is the radius parameter which, in principle, is related to the size of the boson source,  $\lambda$  is a parameter that reflects the strength of the quantum statistics effect as well as the degree to which the Gaussian function fits to the correlation function, and  $\alpha$  is an overall normalization parameter. For the full effect of quantum statistics and a perfect Gaussian fit to the correlation function,  $\lambda$  has the value of unity. Eq. 9 is the same function as used by ALICE to extract  $R$  and  $\lambda$  from quantum statistics in their measurements.

Cuts on charged particle multiplicity ( $N_{ch}$ ), transverse momentum ( $p_T$ ), pseudorapidity ( $\eta$ ), pair transverse momentum ( $k_T = |\vec{p}_a + \vec{p}_b|/2$ ) and  $q_{\text{inv}}$  are applied to the model particles to duplicate those made by ALICE in their measurements. Also, as done by ALICE, like-charge pairs of both signs are summed for pions and charged kaons, and for neutral kaons all pair combinations of  $K^0$  and  $\overline{K}^0$  are summed.

### 3. Results and Discussion

Figure 1 shows sample correlation functions from  $\sqrt{s} = 7$  TeV proton-proton collisions for charged pions, charged kaons, and neutral kaons from the model calculated from Eq. 8. The range in  $N_{ch}$  is 1-11 and  $\tau_{had} = 0.4$  fm/c. Fits of Eq. 9 to the model points are also shown. As seen,  $R \sim 1$  fm, as would be expected for proton-proton collisions, and  $\lambda$  is significantly less than the idealized case of unity. In all three plots, the correlation function is seen to be more exponential in shape than Gaussian which has a significant effect on lowering  $\lambda$ . In addition, for the pion plot, the intercept of the correlation function is itself less than unity due to the effect of the long-lived resonances  $\eta$  and  $\eta'$  diluting the strength of the correlation function.

Figure 2 shows a comparison of the model source parameters using  $\tau_{had} = 0.4$  fm/c with ALICE measurements in two charged particle multiplicity ranges:  $N_{ch}$  1-11 and  $N_{ch} > 11$  [7, 8, 9]. The error bars are statistical+systematic for the ALICE points and are statistical but equal to or less than the marker size for the model points. The approximate scales of the

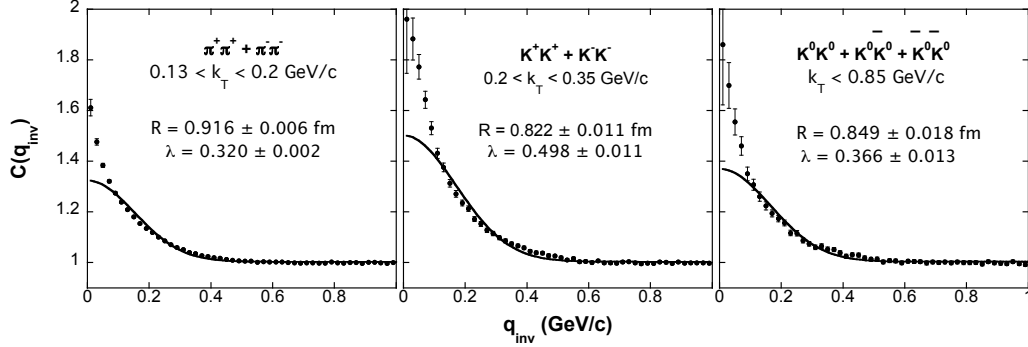


Figure 1: Sample correlation functions from  $\sqrt{s} = 7$  TeV proton-proton collisions for charged pions, charged kaons, and neutral kaons from the model using Eq. 8.  $N_{ch}$  is in the range 1-11 and  $\tau_{had} = 0.4$  fm/c. Fits of Eq. 9 to the model points are also shown.

ALICE  $\lambda$  parameters for pions are indicated by the dashed lines [16], since the specific values were not published by ALICE in Ref. [7]. Although there are specific differences seen between the model and ALICE, overall the model points describe the gross features of the ALICE measurements for pions and charged and neutral kaons reasonably well for both  $R$  and  $\lambda$ : 1) the overall scales of  $R$  for the different particle types agree with ALICE, 2) the model reproduces the increase in  $R$  in going from lower to higher  $N_{ch}$  as measured by ALICE, and 3) the model reproduces the scales of the measured  $\lambda$  parameters. The dependence on  $\tau_{had}$  of the agreement of the model with ALICE was studied and it was found that  $\tau_{had} = 0.4$  fm/c gave the best agreement. For  $\tau_{had} < 0.4$  fm/c the initial density of particles of the system is higher, as suggested by Eqs. 4 and 5, resulting in more rescattering and thus larger  $R$  values, whereas for  $\tau_{had} > 0.4$  fm/c the initial density is lower but the overall timescale is higher again producing larger  $R$  values. From this study the uncertainty in  $\tau_{had}$  is estimated, giving the best value  $\tau_{had} = 0.4 \pm 0.1$  fm/c. This value is in agreement with the upper limit estimate given in Eq. 2.

It is interesting to study the effect that rescattering has on the model source parameters. Figure 3 shows a similar comparison of the model with ALICE as shown in Figure 2 except that rescattering is turned off in the model (decays are still allowed). As seen, while the model agreement with ALICE for  $\lambda$  is not affected much by turning off rescattering, the model  $R$  parameters are strongly affected in that they no longer depend on  $N_{ch}$  and

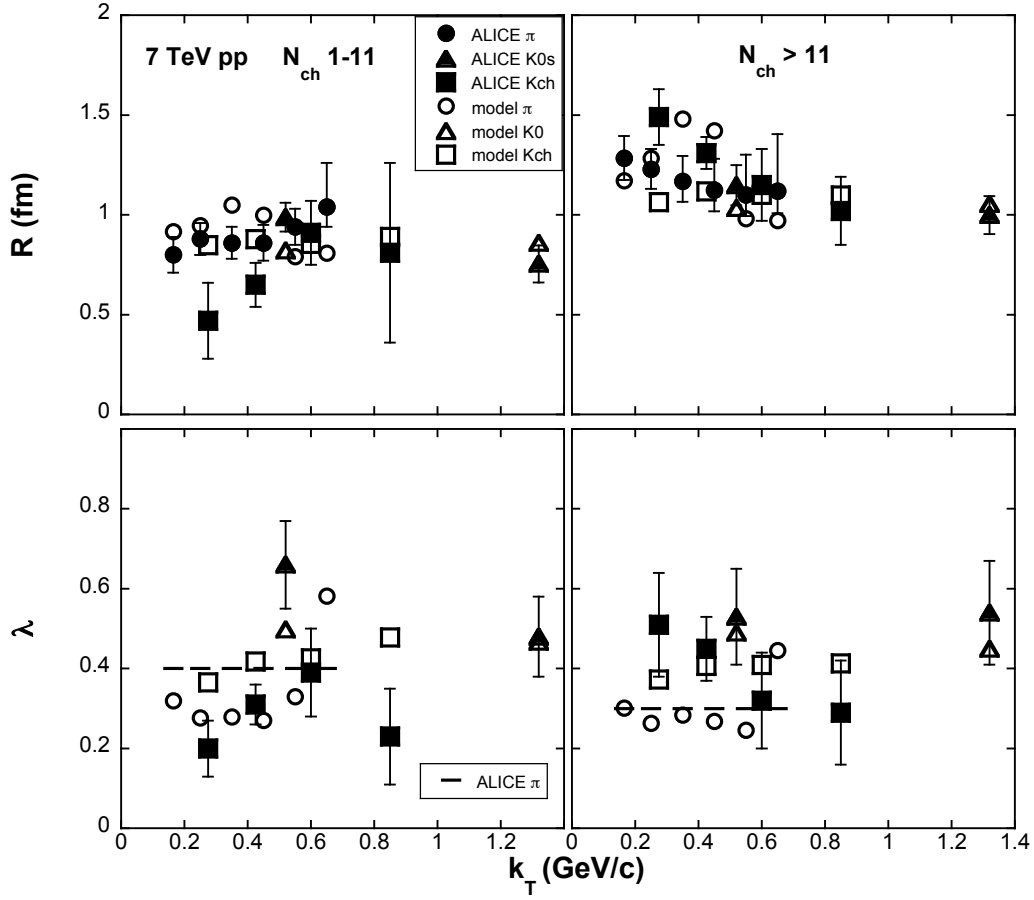


Figure 2: Comparison of source parameters from the model using  $\tau_{had} = 0.4$  fm/c with ALICE measurements in two charged particle multiplicity ranges.

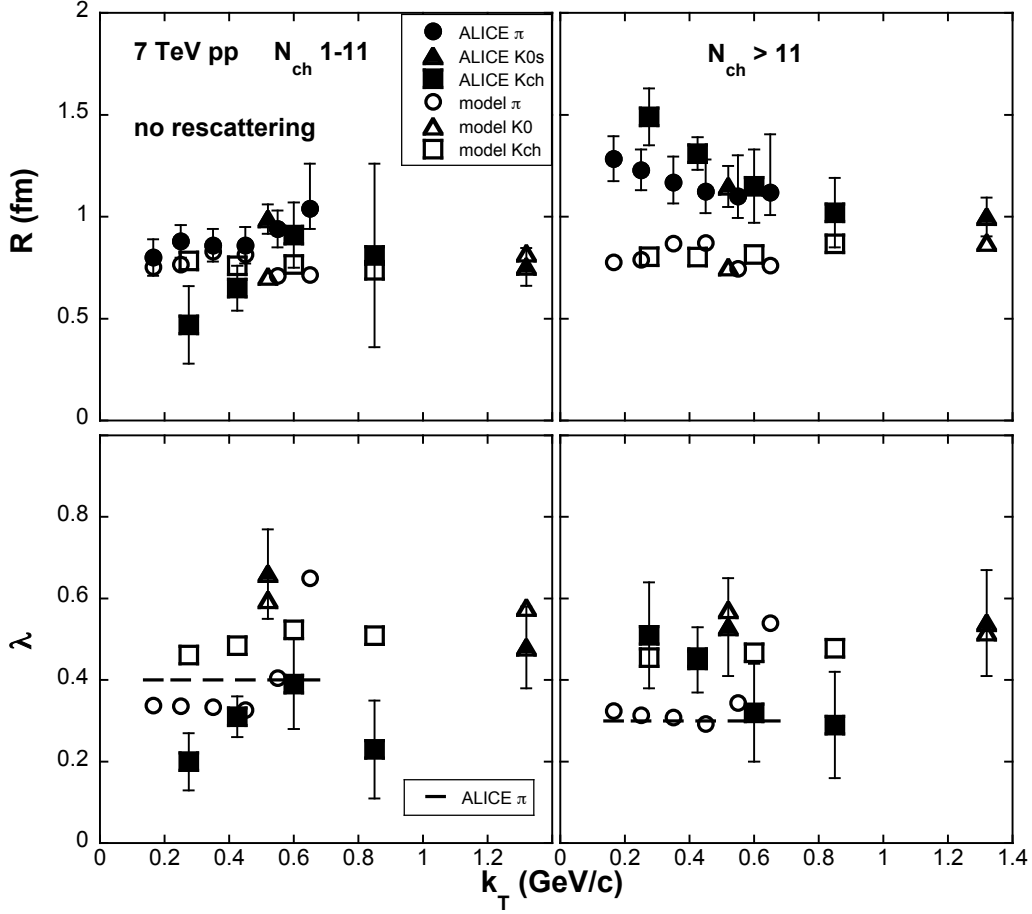


Figure 3: Same as Figure 2 but with rescattering turned off in the model.

are significantly smaller than ALICE for  $N_{ch} > 11$ . This suggests that some kind of “collective motion” of the system, in the present model being due to rescattering, is needed to explain the measured  $N_{ch}$  behavior of  $R$  in  $\sqrt{s} = 7$  TeV proton-proton collisions. The existence of collective behavior in proton-proton collisions has also been suggested in other works [17, 18, 19, 20].

The model connections between the extracted  $R$  and  $\tau_{had}$  values and the underlying physical sizes and timescales in the collision frame are shown in Figure 4. The short-dashed lines represent the equivalent Gaussian widths of the freeze-out time distributions and the solid lines represent the equivalent Gaussian widths of the freeze-out radius distributions. The freeze-out time



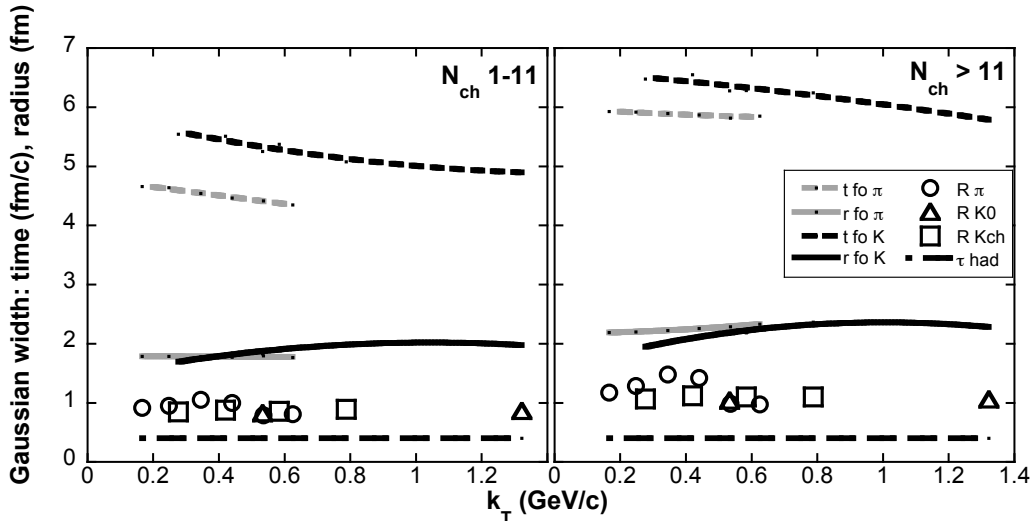


Figure 4: Model comparisons between  $R$  and  $\tau_{had}$  and Gaussian widths of the source radius and time distributions.

and radius width calculations are restricted to the ranges  $t_{FO} < 20$  fm/c and  $r_{FO} < 20$  fm, respectively, to exclude the trivially large timescales and sizes which would be introduced by long-lived resonances. Pions (grey lines) and the combined kaons (black lines) are plotted separately. The model  $R$  parameters are the same as plotted in Figure 2. As seen, although the extracted  $R$  and  $\tau_{had}$  are  $\sim 1$  fm and 0.4 fm/c, respectively, the underlying physical sizes and timescales are  $\sim 2\times$  and  $\sim 15\times$  larger, respectively. The large physical sizes and timescales are due to a combination of time dilation in the initial state, resonance decays and rescattering dynamics. It is also seen that the increase in the  $R$  parameters in going from lower to higher  $N_{ch}$  is also reflected in an increase in the physical radii and timescales for pions and kaons, this effect being completely driven in the model by rescattering, as already suggested in comparing Figures 2 and 3.

Figure 5 shows the time evolution of the energy density at midrapidity,  $\epsilon_{mid}$ , for the first 5 fm/c from the model averaged over all multiplicities for  $\tau_{had} = 0.4$  fm/c. Besides the expected decrease in  $\epsilon_{mid}$  as time evolves due to the expansion of the system, it is seen that  $\epsilon_{mid} > 1$  for  $t < 1.35$  fm/c, reaching  $\epsilon_{mid} \approx 2.4$  GeV/fm<sup>3</sup> at the initial time in the collision. An estimate of the initial energy density in  $\sqrt{s} = 7$  TeV proton-proton colli-

sions based on hydrodynamic calculations has been carried out in Ref. [21], and it is also found there that energy densities greater than  $1 \text{ GeV}/\text{fm}^3$  are initially produced in these collisions, suggesting that a non-hadronic state may be present at the early stages, as is thought to be the case in high-energy heavy-ion collisions. In this scenario, the collision evolves from an initial hydrodynamic state made up of partons into the hadronic state with some possible rescattering and finally to freeze-out from which experimental observables are constructed. In this case, one would expect that collective effects seen in the observables would be due to some combination of hydrodynamics of the partons and final-state hadronic rescattering. The possibility of this hydrodynamic scenario leads to questioning the validity of a purely hadronic picture as is used in the present work which serves as a “limiting case” picture. If a partonic state is indeed initially present, it must evolve eventually into hadrons, and this evolution would likely be gradual in time as opposed to a sudden hadronization of the system as would happen in a first-order phase transition. The simple hadronic rescattering picture could have some degree of validity during this mixed-phase transition period when perhaps “quasi-hadrons” are present. Even at the earliest times when the system may be purely partonic and thus better described by a hydrodynamic picture, hadronic rescattering is perhaps able to mimic to some degree the early hydrodynamic evolution. Thus, in this partonic scenario the present purely hadronic rescattering model might be thought of as mimicking a “viscous” hydrodynamic evolution of the system.

#### 4. Summary

In this work, a hadronic rescattering model with the proper hadronization time width as the free parameter was compared with charged pion and charged and neutral kaon femtoscopy measurements from the LHC ALICE experiment for  $\sqrt{s} = 7 \text{ TeV}$  proton-proton collisions. Comparisons between the model and measurements were made for one-dimensional source parameters in several charged multiplicity and transverse particle pair momentum bins. It is found that a reasonable description of the measured source parameters by the model is obtained for a hadronization proper time width of  $0.4 \pm 0.1 \text{ fm}/c$ , which is in agreement with the estimated upper limit based on the uncertainty principle given in Eq. 2. The model calculations also suggest that 1) some sort of collectivity is necessary to describe the multiplicity dependence of the measured radius parameters, and 2) the underlying

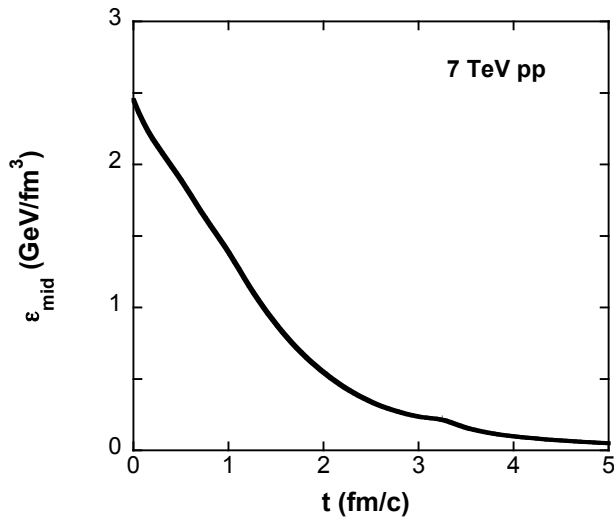


Figure 5: Time evolution of the energy density at midrapidity for the first 5 fm/c from the model averaged over all multiplicities for  $\tau_{had} = 0.4$  fm/c.

physical size and timescale of the collision is significantly larger than what the extracted radius parameters and hadronization proper time width would suggest. It will be interesting to repeat this study once new data are available from the upgraded LHC for  $\sqrt{s} = 14$  TeV proton-proton collisions since the anticipated higher particle multiplicities produced in these collisions should enhance the amount of collectivity present and thus enhance the magnitude of the effects studied in the present work. It would also be of value in characterizing the early stages of these collisions to study penetrating probes such as direct photons and dileptons [21] to obtain direct information on the source of the collectivity suggested in these femtoscopy studies.

The author wishes to acknowledge financial support from the U.S. National Science Foundation under grant PHY-1307188, and to acknowledge computing support from the Ohio Supercomputing Center.

## References

- [1] T. Csörgő, Phys. Lett. B **347**, 354 (1995).
- [2] T. Chmaj, Acta Phys. Polon. **B18**, 1131 (1987).

- [3] T. J. Humanic, AIP Conf. Proc. **1182**, 767-770 (2009) [arXiv:0902.0932v1[nucl-th]].
- [4] D. Truesdale and T. J. Humanic, J. Phys. G: Nucl. Part. Phys. **39**, 015011 (2012).
- [5] T. J. Humanic, Phys. Rev. C **76**, 025205 (2007).
- [6] Q. Li, G. Graf, M. Bleicher, J. Phys. **420**, 012039 (2013).
- [7] K. Aamodt *et al.* [ALICE Collaboration], Phys. Rev. D **84**, 112004 (2011) [arXiv:1101.3665 [hep-ex]].
- [8] B. Abelev *et al.* [ALICE Collaboration], Phys. Rev. D **87**, 052016 (2013) [arXiv:1212.5958 [hep-ex]].
- [9] B. Abelev *et al.* [ALICE Collaboration], Phys. Lett. B **717**, 151 (2012) [arXiv:1206.2056 [hep-ex]].
- [10] T. Sjostrand, L. Lonnblad, S. Mrenna and P. Skands, JHEP **0605**, 026 (2006) [arXiv:hep-ph/0603175 (March 2006)].
- [11] G. Aad et al. [ATLAS Collaboration], Phys. Rev. D **85**, 012001 (2012).
- [12] V. Khachatryan et al. [CMS Collaboration], JHEP **05**, 064 (2011).
- [13] CMS Collaboration, Eur. Phys. J. C **72**, 2164 (2012).
- [14] F. Wang, M. Nahrgang, and M. Bleicher, Phys. Rev. C **85**, 031902(R) (2012).
- [15] Y. Lu and R. D. Amado, Phys. Lett. B **357**, 446-450 (1995) [arXiv:hep-ph/9504362v1 (1995)].
- [16] A. Kisiel, private communication.
- [17] P. Bozek, Acta Phys. Polon. **B41**, 837 (2010) [arXiv:0911.2392 [nucl-th]].
- [18] K. Werner, K. Mikhailov, I. Karpenko, T. Pierog, arXiv:1104.2405 [hep-ph] (2011).
- [19] A. Kisiel, Phys. Rev. C **84**, 044913 (2011) [arXiv:1012.1517 [nucl-th]].

- [20] Z. Chajecki and M. Lisa, Nucl. Phys. A **830**, 199C (2009) [arXiv:0907.3870 [nucl-th]].
- [21] M. Csanád and T. Csörgő, Proc. EDS Blois 2013, Saariselkä, Finland, contribution no. 53 (2013) [arXiv:1307.2082v2 [hep-ph]].